A Product of Ozonolysis of Cholesterol Alters the Biophysical Properties of Phosphatidylethanolamine Membranes†

Ellen Wachtel,‡ Diana Bach,§ Raquel F. Epand,|| Arye Tishbee,‡ and Richard M. Epand*,||

Department of Biochemistry and Biomedical Sciences, McMaster University, Hamilton, Ontario L8N 3Z5, Canada, and Department of Biological Chemistry and Chemical Research Infrastructure Unit, Weizmann Institute of Science, Rehovot, Israel

Received August 23, 2005; Revised Manuscript Received December 5, 2005

ABSTRACT: There is evidence that some products of the reaction of ozone with cholesterol contribute to atherosclerosis. One of these compounds is 3β-hydroxy-5-oxo-5,6-secocholestan-6-al. We have synthesized this compound and have demonstrated that it reacts with phosphatidylethanolamine to form a Schiff base. The 3β-hydroxy-5-oxo-5,6-secocholestan-6-al also affects the physical properties of phosphatidylethanolamines. We show by both DSC and X-ray diffraction that it increases the negative curvature of the membrane. In addition, 3β-hydroxy-5-oxo-5,6-secocholestan-6-al causes the lamellar phase to become disorganized, resulting in the loss of lamellar periodicity. The chemical and physical interactions of 3β-hydroxy-5-oxo-5,6-secocholestan-6-al with phosphatidylethanolamines may contribute to damaging effects of this lipid on cell membranes, resulting in pathology.

It has been known for several years that oxidation of lipids in low-density lipoprotein is involved in atherosclerosis (*1*). There are likely to be a variety of reactive oxygen species and several oxidation products of their reaction with lipids and proteins. There has been recent particular interest in the possible role of ozone in atherogenesis (*2*). Ozone is among the most reactive of the "reactive oxygen species". In addition to its presence as an environmental pollutant, it is also generated in the antibody-catalyzed water oxidation pathway as part of the immune reaction (*3*). It has been shown that the product of the reaction of ozone with cholesterol is present in atherosclerotic plaques (*4*). Products of the oxidation of cholesterol by ozone have also been found in lung tissue, possibly from exposure of lung surfactant to the atmosphere (*5*−*7*). In addition, such cholesterol oxidation products have been found in the brains of autopsy specimens from Alzheimer's patients (*8*, *9*). The ozonolyzed cholesterol accelerates amyloidogenesis in these patients.

Several of the reaction products of the oxidation of cholesterol with ozone contain ketone and aldehyde groups. These functional groups are known to react with compounds containing amino groups to form a Schiff base (*10*). It has been shown that products of the reaction of ozone and cholesterol form Schiff bases with the amino groups of proteins found in atherosclerotic plaques (*4*) as well as with the Abeta protein in Alzheimer's disease, causing this protein to misfold and aggregate (*8*, *9*).

Cholesterol and its initial oxidation products are insoluble in water and are all found in biological membranes in different proportions. The cholesterol oxidation products containing aldehydes or ketones will react with amino groups. In addition to reaction with amino groups of proteins, these oxidized forms will also react with amino lipids that form a major fraction of the lipid components of biological membranes. In the present work we study the reactivity of one of the products of ozonolysis of cholesterol, 3β-hydroxy-5-oxo-5,6-secocholestan-6-al (designated in the following as 4a;[1] Figure 1), with phosphatidylethanolamine, as well as the consequences of formation of this product on the physical properties of the membrane.

EXPERIMENTAL PROCEDURES

Materials. Phospholipids were purchased from Avanti Polar Lipids (Alabaster, AL). Cholesterol was from NuChek Prep (Elysian, MN). The cholesterol ozonolysis product 3β-hydroxy-5-oxo-5,6-secocholestan-6-al (4a; Figure 1) was synthesized in the Chemical Research Infrastructure Unit of the Weizmann Institute of Science following the procedure of Wentworth et al. (*4*). The identity of the compound was verified by mass spectrometry (MS) and ^{1}H NMR analysis. Cholesterol and 4a were stored in the dry state in the dark at −20 °C. After a year and a half, we detected, by high-resolution MS, traces of oxidized 4a. The conversion of aldehyde to acid was quantified by ^{1}H NMR to affect approximately 2.5% of the product.

† This work was supported by a grant from the Canadian Institutes of Health Research (Grant MOP-7654).

* Corresponding author. Tel: 905-525-9140 ext 22073. Fax: 905-521-1397. E-mail: epand@mcmaster.ca.

‡ Chemical Research Infrastructure Unit, Weizmann Institute of Science.

§ Department of Biological Chemistry, Weizmann Institute of Science.

|| Department of Biochemistry and Biomedical Sciences, McMaster University.

[1] Abbreviations: 4a, 3β-hydroxy-5-oxo-5,6-secocholestan-6-al; DSC, differential scanning calorimetry; POPE, 1-palmitoyl-2-oleoylphosphatidylethanolamine; DEPE, dielaidoylphosphatidylethanolamine; T_M, gel to liquid crystalline phase transition temperature; T_H, lamellar to hexagonal phase transition temperature; H_M, gel to liquid crystalline phase transition calorimetric enthalpy; H_H, lamellar to hexagonal phase transition calorimetric enthalpy; MS, mass spectrometry; MSMS, tandem mass spectrometry; TLC, thin-layer chromatography; ^{1}H NMR, proton nuclear magnetic resonance spectroscopy.

10.1021/bi0516778 CCC: $33.50
Published on Web 01/07/2006

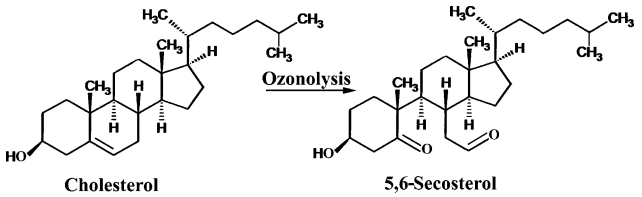

FIGURE 1: Conversion of cholesterol to 4a, a 5,6-secosterol.

^{1}H NMR Spectroscopy. For these measurements dry 4a was dissolved in $CDCl_3$. The spectra were acquired using an Avance 500 spectrometer (Bruker, Rheinstetten, Germany).

Preparation of Lipid Films Containing Sterol and Phospholipid. Phospholipid/sterol mixtures were prepared by mixing appropriate volumes of the lipid solutions in chloroform/methanol (2:1). The solvents were driven off by a stream of nitrogen, and the samples were kept for 3 h under high vacuum.

Visible Spectroscopy. Water (0.5 mL) was added to dry POPE, dry 4a, or a dry mixture of POPE and 4a at a molar ratio of 1:1 (prepared as above). Although salt solutions are generally used in X-ray and DSC measurements, it is preferable to avoid the presence of salt for these spectroscopic measurements. The samples were incubated at 50 °C with frequent vortexing for 0.5 h. The samples were then frozen, and the water was removed by lyophilization. The resulting dry powders were dissolved in 1.5 mL of ethanol. Unlike aqueous suspensions, the lipids were soluble in ethanol, allowing spectroscopic measurement. The absorption spectra of the three samples were measured in the wavelength range of 300−700 nm (Ultraspec 2100 pro UV/visible spectrophotometer; Amersham Biosciences).

Mass Spectrometry and Tandem Mass Spectrometry. Following the spectral measurements, mass spectrometry analysis of the mixture was performed on a Waters Micromass Q-TOF mass spectrometer (Waters-Micromass, Milford, MA) operating in ESI^-, W optic mode with Lockspray. The experimental conditions were as follows: desolvation temperature, 350 °C; source temperature, 100 °C; nitrogen flow, 600 L/h; capillary voltage, 2.8 kV; sampling cone, 30 V; extraction cone, 5.1 V; collision energy, 3 V; scan time, 1 s; scan delay, 0.1 s; mass range, 100−1200. For the MSMS measurements, collision energy was set at 30 V. All other experimental parameters were kept unchanged.

Preparative Thin-Layer Chromatography (TLC). A lipid film containing 50 mol % each of POPE (2.2 μmol) and 4a (2.2 μmol) was hydrated by vortexing with 1 mL of 1 mM Hepes buffer, pH 7, and incubated for 30 min at 50 °C. A tube containing the same amount of POPE alone was treated in the same way. The suspensions were frozen in liquid nitrogen and lyophilized overnight. The ethanolic solutions of POPE and the mixtures were applied in their entirety, as streaks, to a silica GF TLC plate (1000 mesh). A spot of 4a alone in chloroform/methanol (2:1) was also applied.

The plate was run in a chromatographic glass chamber, equilibrated overnight with a running solvent of chloroform/methanol/water (65:25:4), and the spots were developed with iodine. The location of the spots was marked, and the iodine on the spots was allowed to fade before scraping them off the plate. Appropriate control and blank spots were also scraped. The silica powder was extracted with 1 mL of ethanol and centrifuged for 5 min at 4000 rpm in a benchtop centrifuge. The solvent was evaporated until dry, and the phosphate assay of Ames (*11*) was used to determine inorganic phosphate. The experiment was repeated using 1 mM ammonium acetate as a volatile buffer at neutral pH, instead of Hepes, with similar results.

Differential Scanning Calorimetry (DSC). For DSC measurements the lipid/sterol mixtures were dispersed in 20 mM PIPES, 1 mM EDTA, and 150 mM NaCl with 0.002% NaN_3, pH 7.40, by intermittent vortexing over a period of 2 min under argon. Measurements were made using a Nano differential scanning calorimeter (Calorimetry Sciences Corp., American Fork, UT). The scan rate was 0.75 °C/min. The features of the design of this instrument have been described (*12*). DSC curves were analyzed by using the fitting program, DA-2, provided by Microcal Inc. (Northampton, MA) and plotted with Origin, version 5.0. With duplicate samples the enthalpies ΔH_M are precise to ±10% and ΔH_H to ±15%. Transition temperatures are precise to ±0.05 °C. The dependence of the transition temperatures on the presence of 4a was determined from a series of DSC scans of five to eight samples. The regression coefficient for the linear dependence of these temperatures on the mole fraction of 4a is given in the figure legends.

X-ray Diffraction. For X-ray diffraction experiments 0.15 M NaCl solution in 0.01 M Tris·HCl buffer (pH 7.4) was added to dry phospholipids or to phospholipid/sterol mixtures to obtain a final concentration of about 10 mg/mL. The dispersions were incubated for 0.5 h at 50 °C with frequent vortexing. After incubation the dispersions were centrifuged in an Eppendorf centrifuge for 15 min. The pellet was loaded into 1.5 mm quartz X-ray capillaries. In the case of the pure sterols or sterol mixtures, the dry powders were dispersed in 0.15 M NaCl in buffer and the dispersions inserted into the X-ray capillaries. Low-angle X-ray diffraction experiments were performed as described by Bach et al. (*13*). Detector resolution (δq/pixel) was 0.003 Å^{-1}, where $q = 4\pi \sin \theta/\lambda$, 2θ is the scattering angle, and λ is 1.54 Å. Cylinder diameters in the hexagonal phase of DEPE/sterol mixtures and POPE/sterol mixtures were calculated as mean values based on the positions of three to five Bragg diffraction peaks (10, 11, 20, 21, and 30) of the two-dimensional hexagonal lattice.

RESULTS

Visible Spectroscopy. Aqueous suspensions of mixtures of POPE or DEPE with 4a at high sterol content are observed to be yellow-green in color following lyophilization, whereas the individual components are white. The intensity of the color deepens when the pellets are heated during X-ray diffraction experiments. Under the same conditions, no color is developed in mixtures of 4a with DOPC, which lacks a primary amine group. In Figure 2 are presented the absorption spectra of POPE, 4a, and POPE/4a (molar ratio 1:1). Neither 4a nor POPE displays absorption maxima in the wavelength range 300−700 nm; however, in the spectrum of the mixture a single peak is observed at ~440 nm. An absorption maximum at this wavelength has been associated with the formation of a Schiff base (*14*). A Schiff base adduct would be formed by reaction between either the aldehyde group and/or the ketone group of 4a and the amine of the POPE headgroup (Figure 3).

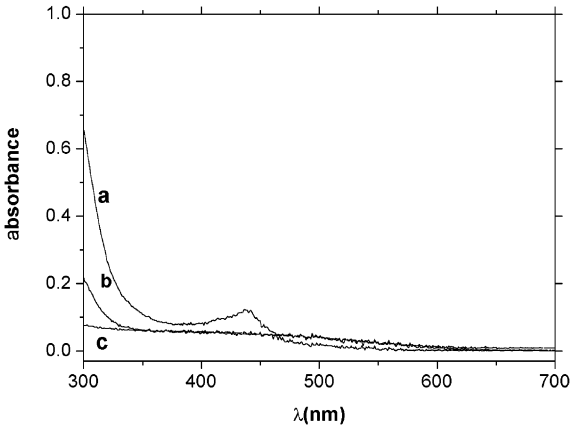

FIGURE 2: Absorption spectra of (a) POPE (2.7 mg)/4a (1.7 mg) (1:1 molar ratio), (b) 4a (1.9 mg) only, and (c) POPE (2.7 mg) only.

High-Resolution Mass Spectrometry. To verify the identity of the reaction product, high-resolution mass spectrometry analysis was performed on the POPE/4a mixture in ethanol. Measurements were made in both the positive and negative ion modes. In the negative mode we observed *m*/*z* values of 417.3357 $[M - H]^-$, a deviation of 1.0 mDa (2.5 ppm) from the composition $C_{27}H_{45}O_3^-$ predicted for 4a; 716.5206 $[M - H]^-$, a deviation of 2.0 mDa (2.7 ppm) from the composition $C_{39}H_{75}NO_8P^-$ predicted for POPE; and 1116.8552 $[M - H]^-$. There was also a peak at 433.3297 that we attribute to the very small fraction of oxidized 4a that was also observed with ^{1}H NMR (see Experimental Procedures section), with a predicted composition $C_{27}H_{45}O_4^-$. Peaks corresponding to 4a and POPE were also observed in the positive ion mode. The peak at 1116.8552 agrees to within −1.8 ppm (−2.0 mDa) with an elemental composition of $C_{66}H_{119}NO_{10}P^-$, i.e., a complex of POPE and 4a minus the mass of a water molecule. This is consistent with the formation of a Schiff base.

To further verify the identification of the Schiff base, tandem mass spectrometry (MSMS) analysis was performed: the peak at 1116.8552 was selected for fragmentation. The following peaks were observed: 716.51 $[M - H]^-$, which coincides with the elemental composition $C_{39}H_{75}NO_8P^-$ predicted for POPE; 281.24 $[M - H]^-$, which coincides with the elemental composition $C_{18}H_{33}O_2^-$ predicted for the oleic acid moiety of the phospholipid; and 255.23 $[M - H]^-$, which coincides with the elemental composition $C_{16}H_{31}O_2^-$ predicted for the palmitic acid moiety of the phospholipid.

The possibility of the formation of a Schiff base between the aldehyde of 4a and amino groups of peptides or proteins has been suggested (*4*, *9*). However, to the best of our knowledge this is the first time that the formation of a Schiff base between 4a and a phospholipid is reported. We consider that such an adduct may be relevant to biological membranes where PE is found at high concentration.

Quantitation of Schiff Base by Preparative TLC. The entire POPE applied to the plate was recovered (by phosphorus determination). The mixture of POPE and 4a produced two spots. One was located at the same position as POPE alone, and the second ran ahead of POPE. This latter spot contained 19−20 nmol of phosphate, approximately 1% of the amount of POPE in the mixture. We associate the spot running ahead of POPE, for the POPE/4a mixture, with the Schiff base. Repeating this experiment using 1 mM ammonium acetate buffer gave about the same amount of product of 4a and POPE as observed with Hepes buffer, indicating that neither the solid residues from the Hepes buffer, deposited after lyophilization, nor the possibility of some reaction with the more nucleophilic ammonia in the ammonium acetate buffer affected the analysis. The latter finding suggests that the reaction takes place between components in the membrane and does not occur as rapidly with substances in the aqueous phase.

DSC. We determined the effect of 4a on the phase transition properties of phosphatidylethanolamines. The family of DSC curves of DEPE with increasing mole fraction of 4a shows that the L_β to L_α transition temperature (T_M) and the L_α to H_{II} phase transition temperature (T_H) decrease (Figure 4). The dependence of T_M, T_H, ΔH_M, and ΔH_H is shown as a function of the mole fraction of 4a (Figure 5). A similar study was done with POPE (Figures 6 and 7).

Low-Angle X-ray Diffraction. We first measured the properties of simple mixtures of 4a and cholesterol, in the absence of phospholipid. The low-angle X-ray diffraction pattern of 4a alone showed no evidence of crystalline diffraction nor did a sample of 0.89 mole fraction of 4a mixed with cholesterol (Figure 8, bottom curve). When the amount of 4a is decreased to 0.45 mole fraction (Figure 8, middle curve), two diffraction peaks are observed, consistent with phase separation. The weaker of the two peaks is at 37 Å while the stronger is at 34 Å. Pure cholesterol has a diffraction peak at 34 Å, indexed as either the 010 of the anhydrous form (*15*) or 001 of the monohydrate (*16*). The lower angle peak is most likely due to a 4a-rich mixture with cholesterol. At a mol fraction of 0.11 of 4a (top trace of Figure 8), a single peak is observed at a *d* spacing of 35 Å, indicating a homogeneous mixture at the resolution of the experiment.

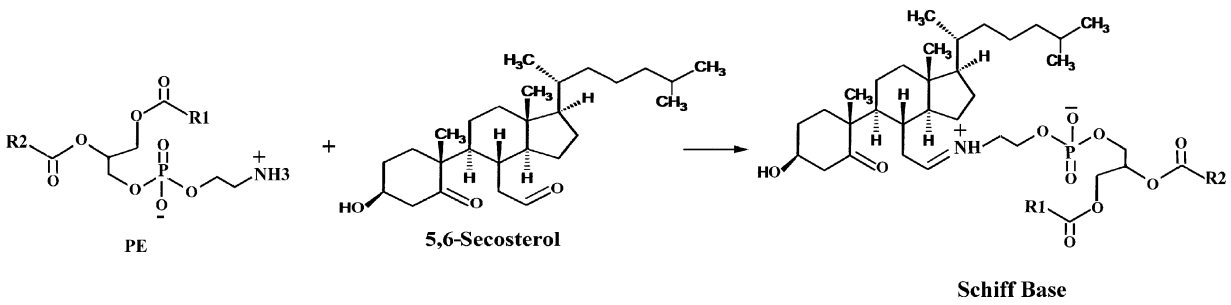

FIGURE 3: Reaction of 4a with a phosphatidylethanolamine to form a Schiff base. Only one of the two possible reaction products is shown for illustration. The other product would also be a Schiff base formed by a similar reaction between the ketone group of 4a and the amino group of phosphatidylethanolamine.

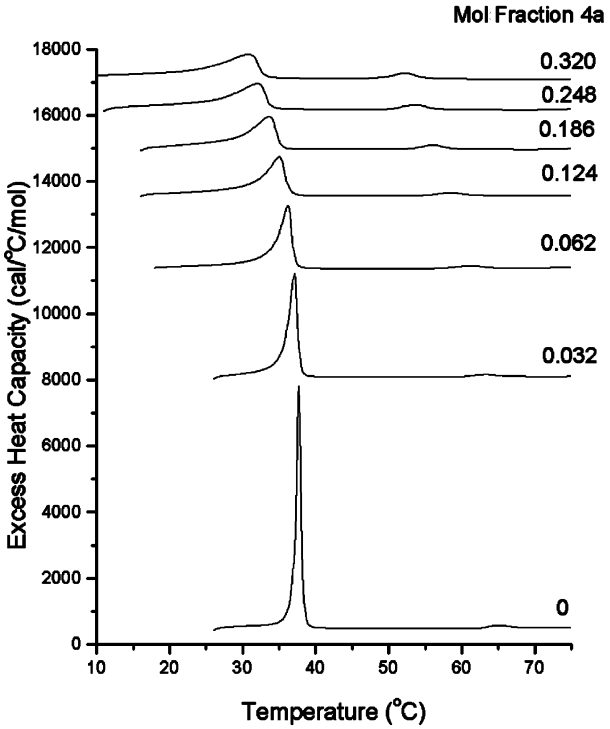

FIGURE 4: DSC heating scans of DEPE in the presence of various mole fractions of 4a, as indicated on the graph. Scan rate = 0.75 °C/min.

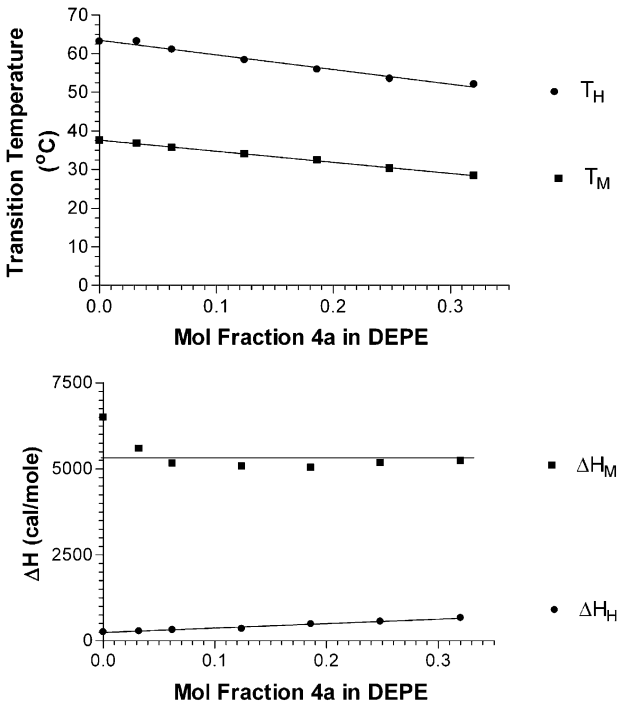

FIGURE 5: Dependence of T_M, T_H, ΔH_M, and ΔH_H of DEPE on the mole fraction of 4a. The linear regression for the change in the main transition temperature with mole fraction is -29 ± 1 ($R^2 = 0.999$) and for the change in the hexagonal phase transition temperature is -38 ± 2 ($R^2 = 0.982$). The average value of ΔH_M was found to be 5400 ± 520 cal/mol.

We also studied mixtures of phosphatidylethanolamine with 4a or with cholesterol, using X-ray diffraction. DEPE dispersed in water exhibits two thermotropic phase transitions: a gel to liquid crystal transition near 37 °C and liquid crystal to hexagonal phase transition at about 65 °C (*17*).

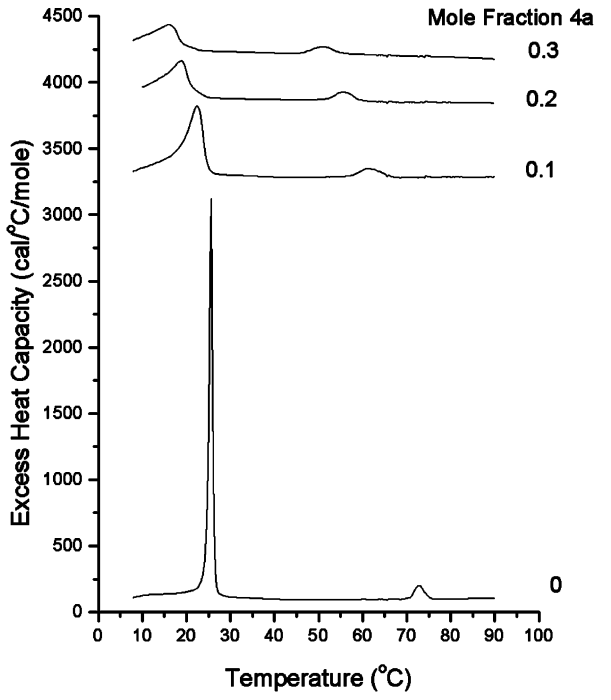

FIGURE 6: DSC heating scans of POPE in the presence of various mole fractions of 4a, as indicated on the graph. Scan rate = 0.75 °C/min.

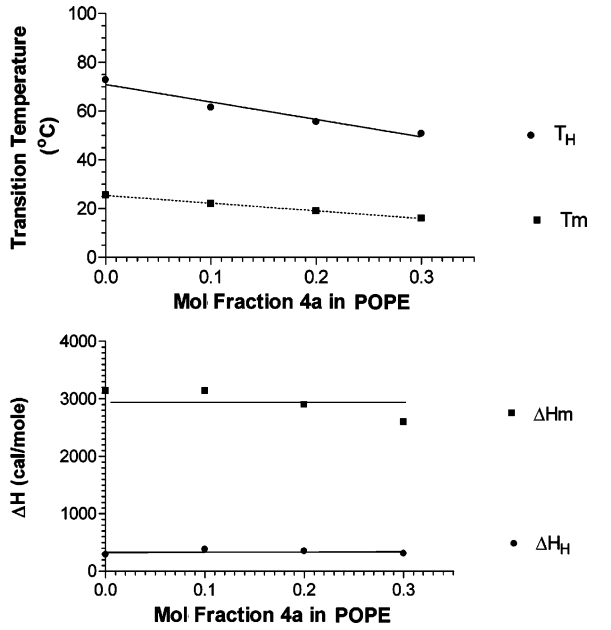

FIGURE 7: Dependence of the transition temperatures T_M (■) and T_H (●) and transition enthalpies ΔH_M (■) and ΔH_H (●) of POPE on the mole fraction of 4a. The linear regression for the change in the main transition temperature with mole fraction is -31.6 ± 1 ($R^2 = 0.988$) and for the change in the hexagonal phase transition temperature is -72 ± 11 ($R^2 = 0.959$).). The average value of ΔH_M was found to be 2950 ± 260 cal/mol and for ΔH_H was found to be 335 ± 40 cal/mol.

The lamellar stacking of DEPE is disrupted above a mole fraction of 4a of ~0.4 in both the gel and liquid crystalline phases. Nevertheless, the hexagonal phase does form at higher temperatures, at least up to a mole fraction of 4a of 0.6. Increasing amounts of 4a reduces the diameter of the hexagonal phase cylinders from ~72 Å in the absence of 4a to ~62 Å at 71 °C with a mole fraction of 0.6 of 4a (Figure

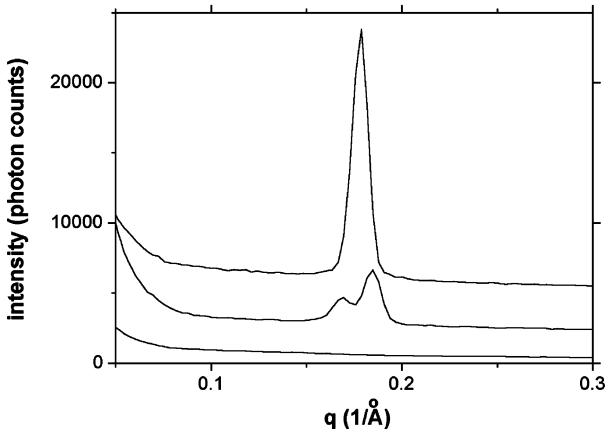

FIGURE 8: Low-angle X-ray diffraction patterns of 4a/cholesterol mixtures in 0.15 M NaCl in buffer: 0.11 mole fraction of 4a (top curve); 0.45 mole fraction of 4a (middle curve); 0.89 mole fraction of 4a (bottom curve). $q = 4\pi \sin \theta/\lambda$, where 2θ is the scattering angle and $\lambda = 1.54$ Å.

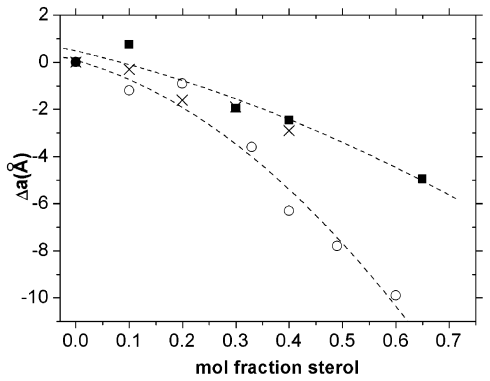

FIGURE 9: Comparison of the change in cylinder diameter (Δa) in the hexagonal phase of DEPE in mixtures with cholesterol (× from ref *18*; ■ from ref *19*) or 4a (○, this work).

9). 4a is more effective than cholesterol in reducing the diameter of the hexagonal phase cylinders, i.e., increasing the negative curvature. [The measurements of the DEPE/cholesterol mixtures were taken from previous publications and were made at 75 °C (*18*), at which temperature $a = 71$ Å for DEPE alone, and at 69 °C (*19*), where $a = 75$ Å.]

Mixtures of POPE with 4a behave very similarly to DEPE/4a mixtures, although the two lipids differ in structure. POPE has one saturated chain and one chain with a single *cis* double bond, rendering the molecule less rigid, with a lower L_α to L_β phase transition temperature. DEPE has one *trans* double bond in each of the two chains that produces a more rigid structure, similar to that of saturated phospholipids. X-ray diffraction measurements show that when cholesterol is mixed with POPE, the interlamellar spacing (d) in the gel state (13 °C) is decreased from 63 to 55 Å up to a mole fraction of cholesterol of 0.62 (Figure 10). In the liquid crystalline state ($T = 38$ °C), the interlamellar spacing is relatively insensitive to the sterol content, $d = 54-55$ Å. Similar behavior is observed when 4a instead of cholesterol is mixed with POPE (Figure 10), except in this case the diffraction peak, due to interlamellar stacking, is observed only until a mole fraction 4a of 0.4. Above this value the presence of 4a obviously disrupts the stacking in both the gel and liquid crystalline phases (Figure 11). The hexagonal phase of POPE forms above 70 °C. Even the disordered POPE/4a mixtures, i.e., mole fraction of 4a greater than 0.4,

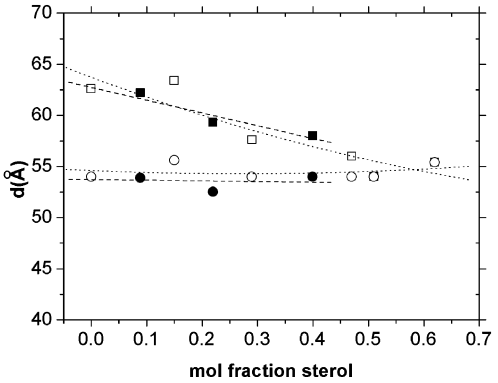

FIGURE 10: Change in the interlamellar spacing of POPE/4a mixtures (closed symbols) and POPE/cholesterol mixtures (open symbols) in the gel state (squares) and the liquid crystal state (circles).

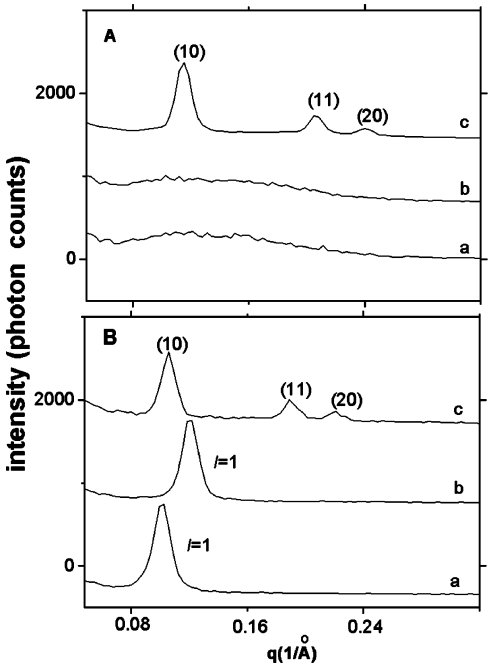

FIGURE 11: X-ray diffraction profiles of (A) POPE/4a mixtures (1:1 molar ratio) at (a) 13 °C, (b) 42 °C, and (c) 71 °C. The Miller indices of the hexagonal phase are noted. (B) POPE alone at (a) 13 °C, (b) 39 °C, and (c) 71 °C. The first-order diffraction peak in the gel and liquid crystal phases is noted as are the Miller indices of the hexagonal phase. $q = 4\pi \sin \theta/\lambda$, where 2θ is the scattering angle and $\lambda = 1.54$ Å.

transform into the hexagonal phase (Figure 11). The diameter of the POPE hexagonal phase cylinder at 71 °C is determined from the X-ray diffraction pattern to be ~71 Å. Increasing amounts of sterol are effective in reducing this diameter, i.e., increasing the negative curvature (Figure 12). However, whereas 0.6 mole fraction of cholesterol reduces the diameter by 5 Å, this value reaches 10 Å for comparable amounts of 4a.

DISCUSSION

The demonstration that phosphatidylethanolamine reacts with 4a has important implications for athererosclerosis, since 4a has been found in atherosclerotic plaques (*4*). 4a is a product of reaction with ozone, a reactive oxygen species that is produced in inflammatory processes (*3*) that are associated with atherosclerosis (*20*−*23*). It has been con-

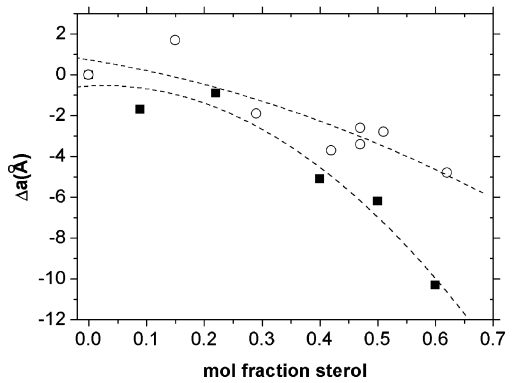

FIGURE 12: Change in the cylindrical diameter (Δa) in the hexagonal phase of POPE in mixtures with cholesterol (○) or 4a (■).

sidered that 4a can react with proteins to form a Schiff base (*8*, *9*). However, it is also likely that other reaction products of ozone and cholesterol that contain aldehyde and/or ketone groups also react with the amino groups of phosphatidylethanolamine, a major lipid component of the cytoplasmic leaflet of the plasma membrane as well as intracellular membranes. It has been shown that other aldehydes and ketones form Schiff bases with phosphatidylethanolamine, such as retinal (*24*) as well as acetaldehyde derived from ethanol metabolism (*25*). In addition, there are a number of examples of aldehyde and ketone oxidation products of lipids that form Schiff bases with phosphatidylethanolamine. These include keto aldehydes and isoketal products of free radical-induced peroxidation of arachidonic acid (*26*); products of plasmalogen oxidation (*27*); 4-hydroxynonenal, a major product of lipid peroxidation of $n - 6$ polyunsaturated fatty acids (*28*); and Schiff base adducts of phosphatidylethanolamine that form in oxidized low-density lipoprotein (LDL) and promote platelet prothrombinase activity (*29*).

The other major amino-containing phospholipid of biological membranes is phosphatidylserine. However, the reactivity of the amino group of phosphatidylserine is lower than that of phosphatidylethanolamine. It has been shown that phosphatidylserine reacts poorly with aldehydes and ketones (*28*), less than phosphatidylethanolamine (*30*). This is in accord with our qualitative observation that there was less reactivity as indicated by less color change when phosphatidylserine was mixed with 4a, compared with phosphatidylethanolamine.

In addition to reacting with phosphatidylethanolamine, 4a also modifies the intrinsic curvature of bilayers containing this lipid. This is indicated both by the lowering of T_H, as measured by DSC (Figures 5 and 7), and by the observed reduction in the diameter of H_{II} phase cylinders measured by X-ray diffraction (Figures 9 and 12). The effect is modest, requiring a relatively high mole fraction of 4a, but the promotion of negative curvature by this oxidized form of cholesterol is greater than that of cholesterol itself. The magnitude of the effect of 4a on membrane curvature is similar for DEPE and for POPE as assessed by both shifts in T_H and changes in hexagonal phase cylinder diameter. Curiously, ΔH_H increases when 4a is added to DEPE (Figure 5), even though the ΔH_H for POPE/4a mixtures is independent of the amount of 4a (Figure 7). The effect of 4a on the ΔH_H of DEPE is similar to the effect of cholesterol (*31*). We have suggested that, as a consequence of the shorter length of cholesterol, addition of the sterol results in more hydrocarbon packing voids in the hexagonal phase resulting in lowered stability and increased bilayer to hexagonal phase transition enthalpy. One would expect less effect of length mismatch with POPE, where the *sn*-1 acyl chain is two carbons shorter and the *sn*-2 acyl chain has a *cis*, rather than *trans*, double bond. This may be the reason why 4a causes little change in the ΔH_H of POPE, although cholesterol still increases the ΔH_H of this lipid (*31*).

Addition of 4a to bilayers in the lamellar phase results in the disordering of the membrane. Thus, the regular lamellar spacing of POPE disappears in the presence of 4a (Figure 11). The observation that a high mole fraction of 4a can be added to DEPE or POPE without greatly broadening the bilayer to hexagonal phase transition observed by DSC or reducing the sharpness of the diffraction peaks of the hexagonal phase for either of these two phosphatidylethanolamines suggests that 4a can incorporate into the highly curved hexagonal phase structure without greatly perturbing it, in contrast to its disordering of the lamellar phase.

Thus, the products of ozonolysis of cholesterol would be expected to alter membrane properties by reacting with phosphatidylethanolamine as well as by altering the stability and curvature properties of the membrane bilayer. These factors may contribute to the atherosclerogenic effects of this lipid oxidation product.

ACKNOWLEDGMENT

We are grateful to Prof. Israel Miller, Department of Biological Chemistry, Weizmann Institute of Science, for many helpful discussions and to Dr. Yoav Barak, Department of Biological Chemistry, Weizmann Institute of Science, for measurement of the visible spectra.

REFERENCES

1. Steinbrecher, U. P., Parthasarathy, S., Leake, D. S., Witztum, J. L., and Steinberg, D. (1984) Modification of low-density lipoprotein by endothelial cells involves lipid peroxidation and degradation of low-density lipoprotein phospholipids, *Proc. Natl. Acad. Sci. U.S.A. 81*, 3883−3887.
2. Loscalzo, J. (2004) Ozone—from environmental pollutant to atherogenic determinant, *N. Engl. J. Med. 350*, 834−835.
3. Wentworth, P., Jr., McDunn, J. E., Wentworth, A. D., Takeuchi, C., Nieva, J., Jones, T., Bautista, C., Ruedi, J. M., Gutierrez, A., Janda, K. D., Babior, B. M., Eschenmoser, A., and Lerner, R. A. (2002) Evidence for antibody-catalyzed ozone formation in bacterial killing and inflammation, *Science 298*, 2195−2199.
4. Wentworth, P., Jr., Nieva, J., Takeuchi, C., Galve, R., Wentworth, A. D., Dilley, R. B., DeLaria, G. A., Saven, A., Babior, B. M., Janda, K. D., Eschenmoser, A., and Lerner, R. A. (2003) Evidence for ozone formation in human atherosclerotic arteries, *Science 302*, 1053−1056.
5. Pryor, W. A., Wang, K., and Bermudez, E. (1992) Cholesterol ozonation products as biomarkers for ozone exposure in rats, *Biochem. Biophys. Res. Commun. 188*, 618−623.
6. Pulfer, M. K., Taube, C., Gelfand, E., and Murphy, R. C. (2005) Ozone exposure in vivo and formation of biologically active oxysterols in the lung, *J. Pharmacol. Exp. Ther. 312*, 256−264.
7. Pulfer, M. K., and Murphy, R. C. (2004) Formation of biologically active oxysterols during ozonolysis of cholesterol present in lung surfactant, *J. Biol. Chem. 279*, 26331−26338.
8. Bieschke, J., Zhang, Q., Powers, E. T., Lerner, R. A., and Kelly, J. W. (2005) Oxidative metabolites accelerate Alzheimer's amyloidogenesis by a two-step mechanism, eliminating the requirement for nucleation, *Biochemistry 44*, 4977−4983.
9. Zhang, Q., Powers, E. T., Nieva, J., Huff, M. E., Dendle, M. A., Bieschke, J., Glabe, C. G., Eschenmoser, A., Wentworth, P., Jr., Lerner, R. A., and Kelly, J. W. (2004) Metabolite-initiated protein

misfolding may trigger Alzheimer's disease, *Proc. Natl. Acad. Sci. U.S.A. 101*, 4752−4757.
10. Reymond, J.-L., and Chen, Y. (1995) Catalytic, enantioselective aldol reaction with an artificial aldolase assembled from a primary amine and an antibody, *J. Org. Chem. 60*, 6970−6979.
11. Ames, B. N. (1966) Assay of inorganic phosphate, total phosphate and phosphatases, *Methods Enzymol. 8*, 115−118.
12. Privalov, G., Kavina, V., Freire, E., and Privalov, P. L. (1995) Precise scanning calorimeter for studying thermal properties of biological macromolecules in dilute solution, *Anal. Biochem. 232*, 79−85.
13. Bach, D., Borochov, N., and Wachtel, E. (2002) Phase separation of cholesterol and the interaction of ethanol with phosphatidylserine-cholesterol bilayer membranes, *Chem. Phys. Lipids 114*, 123−130.
14. Bazhulina, N. P., Morozov, Y. V., Papisova, A. I., and Demidkina, T. V. (2000) Pyridoxal 5′-phoshate schiff base in *Citrobacter freundii* tyrosinephenol-lyase. Ionic and tautomeric equilibria, *Eur. J. Biochem. 267*, 1830−1836.
15. Shieh, H. S., Hoard, L. G., and Nordman, C. E. (1977) Crystal structure of anhydrous cholesterol, *Nature 267*, 287−289.
16. Craven, B. M. (1976) Crystal structure of cholesterol monohydrate, *Nature 260*, 727−729.
17. Epand, R. M. (1985) Diacylglycerols, lysolecithin, or hydrocarbons markedly alter the bilayer to hexagonal phase transition temperature of phosphatidylethanolamines, *Biochemistry 24*, 7092−7095.
18. Takahashi, H., Sinoda, K., and Hatta, I. (1996) Effects of cholesterol on the lamellar and the inverted hexagonal phases of dielaidoylphosphatidylethanolamine, *Biochim. Biophys. Acta 1289*, 209−216.
19. Cheetham, J. J., Wachtel, E., Bach, D., and Epand, R. M. (1989) Role of the stereochemistry of the hydroxyl group of cholesterol and the formation of nonbilayer structures in phosphatidylethanolamines, *Biochemistry 28*, 8928−8934.
20. Foley, S. M. (2005) Update on risk factors for atherosclerosis: the role of inflammation and apolipoprotein E, *Medsurg. Nurs. 14*, 43−50.
21. Hansson, G. K. (2005) Inflammation, atherosclerosis, and coronary artery disease, *N. Engl. J. Med. 352*, 1685−1695.
22. Meng, C. Q. (2005) Inflammation in atherosclerosis: new opportunities for drug discovery, *Mini. Rev. Med. Chem. 5*, 33−40.
23. Mullenix, P. S., Andersen, C. A., and Starnes, B. W. (2005) Atherosclerosis as inflammation, *Ann. Vasc. Surg. 19*, 130−138.
24. Fishkin, N. E., Sparrow, J. R., Allikmets, R., and Nakanishi, K. (2005) Isolation and characterization of a retinal pigment epithelial cell fluorophore: an all-trans-retinal dimer conjugate, *Proc. Natl. Acad. Sci. U.S.A. 102*, 7091−7096.
25. Kenney, W. C. (1984) Formation of Schiff base adduct between acetaldehyde and rat liver microsomal phosphatidylethanolamine, *Alcohol Clin. Exp. Res. 8*, 551−555.
26. Bernoud-Hubac, N., Fay, L. B., Armarnath, V., Guichardant, M., Bacot, S., Davies, S. S., Roberts, L. J., and Lagarde, M. (2004) Covalent binding of isoketals to ethanolamine phospholipids, *Free Radical Biol. Med. 37*, 1604−1611.
27. Stadelmann-Ingrand, S., Pontcharraud, R., and Fauconneau, B. (2004) Evidence for the reactivity of fatty aldehydes released from oxidized plasmalogens with phosphatidylethanolamine to form Schiff base adducts in rat brain homogenates, *Chem. Phys. Lipids 131*, 93−105.
28. Guichardant, M., Taibi-Tronche, P., Fay, L. B., and Lagarde, M. (1998) Covalent modifications of aminophospholipids by 4-hydroxynonenal, *Free Radical Biol. Med. 25*, 1049−1056.
29. Zieseniss, S., Zahler, S., Muller, I., Hermetter, A., and Engelmann, B. (2001) Modified phosphatidylethanolamine as the active component of oxidized low-density lipoprotein promoting platelet prothrombinase activity, *J. Biol. Chem. 276*, 19828−19835.
30. Fountain, W. C., Requena, J. R., Jenkins, A. J., Lyons, T. J., Smyth, B., Baynes, J. W., and Thorpe, S. R. (1999) Quantification of N-(glucitol)ethanolamine and N-(carboxymethyl)serine: two products of nonenzymatic modification of aminophospholipids formed in vivo, *Anal. Biochem. 272*, 48−55.
31. Epand, R. M., and Bottega, R. (1987) Modulation of the phase transition behavior of phosphatidylethanolamine by cholesterol and oxysterols, *Biochemistry 26*, 1820−1825.

BI0516778